Optical measurement of doping efficiency in poly(3-hexylthiophene) solutions and thin films

Chenchen Wang, Duc T. Duong, Koen Vandewal, Jonathan Rivnay, and Alberto Salleo

Phys. Rev. B **91**, 085205 — Published 17 February 2015

DOI: 10.1103/PhysRevB.91.085205

Optical measurement of doping efficiency in Poly(3-hexylthiophene) solutions and thin films

Chenchen Wang,[1] Duc T. Duong,[2] Koen Vandewal,[3] Jonathan Rivnay[4] and Alberto Salleo[2]

[1]*Department of Applied Physics, Stanford University, Stanford, CA 94305, USA*

[2]*Department of Materials Science and Engineering, Stanford University, Stanford, CA 94305, USA*

[3]*Institut für angewandte Photophysik, Dresden University of Technology, Dresden, Germany*

[4]*Department of Bioelectronics, École Nationale Supérieure des Mines, CMP-EMSE, MOC, 13541, France*

Abstract

The doping mechanism of 2,3,5,6-tetrafluoro-7,7,8,8,-tetracyanoquinodimethane (F4TCNQ) doped poly(3-hexylthiophene) (P3HT) thin films and solutions is studied by UV-visible and IR absorption spectral analysis. We show that integer charge transfer between the two molecules is observed in this system with 63% of the dopants producing a fully transferred charge in thin film. The primary P3HT doped species in solution and thin film are shown to be bipolarons and polarons, respectively. The absorption signatures of polarons and bipolarons are identified and their cross sections are measured, which can be used to evaluate the influence of processing conditions on the density of impurity dopant-induced polarons in nominally 'neat' P3HT films.

PACS number(s): 81.05.Fb, 82.35.Cd

Introduction

Doping is one of the most ubiquitous methods used to modulate the electronic properties of semiconductors and is widely applied in a variety of electronic devices.[1–4] In order to design optimal organic semiconductor based devices, one of the key issues is the ability to fabricate well-defined p- or n-type doped layers with these materials. In contrast to doping in silicon, where substitutional impurities generate electron donating or accepting states within the bandgap, dopants for organic semiconductors are typically strong oxidizers or reducers and doping occurs via a chemical charge transfer process without altering the covalent bonding in the semiconductor.[5–7] P-type doping, for instance, involves introducing an acceptor molecule with a lowest unoccupied molecular orbital (LUMO) lower in energy than that of the highest occupied molecular orbital (HOMO) of the donor, which results in an electron transfer between the dopant and the host material.[8–10] Over the past few decades, many studies have been aimed towards understanding such doping processes, many of which focused on answering two questions: what is the nature of the generated charge (polarons, bipolarons, free carriers or is a strongly bound complex formed) and how efficiently does a dopant molecule generate these species. These two questions are widely discussed but not yet completely answered.

The complexity and diversity of organic materials suggests a material dependent mechanism. Even in one of the most frequently studied systems, which involves the p-type doping of poly(3-hexylthiophene) (P3HT) with 2,3,5,6-Tetrafluoro-7,7,8,8-tetracyanoquinodimethane (F4TCNQ), the doping mechanism remains unclear. Recently, first principles calculations have suggested that both donor and acceptor molecules form a bound complex and only partial charge transfer occurs between these two molecules.[11] Similar results were also reported for F4TCNQ-doped pentacene, where Salzmann et al. provided experimental evidence for the existence of intermolecular hybrids and suggested that the LUMO of such a complex introduces doping states within the semiconductor's bandgap, resulting in a thermally activated carrier generation process.[12] In many cases, however, a redox model is used wherein a single electron is transferred from P3HT to

F4TCNQ leading the formation of charge carriers in the form of either polarons or bipolarons. Fortunately, regardless of which model is chosen, doping generally introduces absorption features in the sub-bandgap region. As a result, optical absorption is a natural characterization tool for the analysis of the doping process.

Although much effort has been put into improving the conductivity of doped P3HT, the typical overall dopant concentration remains high compared to conventional inorganic doping. Up to 10-20 wt% F4TCNQ, for instance, is required to achieve sheet resistances of 0.1-1 S/cm in P3HT.[5,13] As a result, these high doping concentrations significantly affect the microstructure and morphology of P3HT thin films, imposing a strong dependence of carrier mobility on doping concentration.[7,14] To characterize the doping process in organic semiconductors, however, conventional Hall effect measurements are ineffective. In addition, high conductivities prevent the determination of thin film hole mobility using differential conductivity measurements carried out in thin film transistors. As a result, determining charge carrier concentrations and doping efficiencies remains extremely challenging. Specialized methods such as capacitance-voltage measurements,[7,15] photoelectron spectroscopy measurements,[16,17] or modeling of transistor pinch-off voltages shifts[18] have been developed to address this problem. However, many of these measurements require specially designed sample fabrication or complicated experimental setups, while others only provide limited, indirect and model-dependent information about doping mechanism. In addition, such electrical measurements do not yield details regarding the efficiency of the charge-transfer process and the nature of the generated carriers.

Optical absorption spectroscopy is a simple yet powerful technique that can be used to qualitatively and quantitatively investigate carrier type and concentration in semiconducting polymers. Colaneri et al, for instance, combined optical absorption with magnetic and electrochemical measurements to determine the type of charge species in electrochemically doped poly(3-methylthiophene) thin films.[19] Ziemelis et al also used optical measurements to determine injected carrier types in metal-insulator-semiconductor structures with poly(3-hexylthienylene).[20] In this work, however, we are

interested in characterizing charged species in *molecularly-doped* semiconducting polymer thin films. More recent works by Pingel et al invested the molecularly doped binary system, F4TCNQ:P3HT, and showed that ionization of the dopant-host pair occurs with > 70% efficiency though only 5% of the generated charges dissociate.[21] The absorption cross-section and type of charge generated in solution and thin films are not investigated, however. Finally, the degree of aggregation/crystallinity and average chain rigidity were recently shown by Gao et al to affect the doping properties of the system. Here we would like to further explore the structure-dependent doping process as it relates to the type of generated charge and the doping efficiency.[22,23]

In this report we describe in detail the use of optical absorption spectroscopy to quantitatively characterize F4TCNQ-doped P3HT in both solution and thin films. The absorption signatures in the sub-bandgap region are identified and decomposed to analyze the doping mechanism and absorption cross section of the relevant species. We also estimated the doping efficiency, defined here as the ratio of charge generated in the polymer to total dopant concentration, in F4TCNQ-doped P3HT films, and are able to optically measure the background charge density, probably due to impurity doping, in nominally undoped films.

Results and Discussion

I. Doping in solution

One of the main sources of complexity in conjugated polymer systems comes from the interaction between different polymer chains within well-ordered crystalline domains. To eliminate some of these intricacies, we first focused on F4TCNQ-doped P3HT in solution (Chlorobenzene, CB) at conditions where the interchain interactions are greatly reduced as indicated by the blue-shifted and featureless absorption spectra of P3HT solutions as compared to thin films. Here we collect solution absorption spectra of doped P3HT under different temperature treatment cycles. For each measurement cycle, the solution was

either heated (80°C~100°C) or cooled (~0°C) over the course of a few minutes and then returned to room temperature before a spectrum was collected. We refer to these as cooling/heating cycles. The total heating/cooling time is on the order of ~20-30 minutes per cycle. It is important to note that the cooling/heating cycles put the solution out of equilibrium: the measurements are taken at different times while the solution re-equilibrates at room temperature. However, because the doping/de-doping process is kinetically slow compared to the measurement time, the system can be considered to be in a quasi-steady state during each optical absorption measurement. The main advantage of this method is that it allows us to change the ionized fraction of the species in a closed system in such a way that the total (neutral and ionized) amounts of P3HT and F4TCNQ are invariant.

From Fig. 1, we can see that the absorption spectra of the doped materials change significantly over the course of each cycle. Cooling increases sub-bandgap absorption and bleaches the π− π polymer absorption (Fig. 1(a)); conversely, when the solution is heated, sub-bandgap absorption decreases and the π−π absorption recovers (Fig. 1(b)). The whole process is reversible: after many cooling and heating cycles, the solution always reverts back to its initial state. These changes in polaronic absorption and chromophore bleaching suggest that changing temperature can control the efficiency with which dopants generate a P3HT cation in solution, as was previously reported.[24]

The absorption features in the UV-visible region are analyzed and used to identify charged species after doping. As shown in Fig. 1(c), the doped solution spectrum can be decomposed into five components. Broad absorption peaks at ~2.7 eV and ~3.2 eV correspond to neutral P3HT and F4TCNQ molecules (orange and green dashed lines).[13] Absorption features at ~1.4 eV and ~1.6 eV have almost identical peak positions and shape as those of $K^+(F4TCNQ)^-$ in acetonitrile previously reported[25] and are attributed entirely to singly charged F4TCNQ anion ($F4TCNQ^-$). The observation of the F4TCNQ anion signal here suggests that integer charge transfer occurs between P3HT and F4TCNQ, and that P3HT cations in solution are likely to form polarons or bipolarons instead of a bound complex with partial charge transfer. The energy and number of

observed optical transitions are unique for different types of charge carriers and, as such, allows us to distinguish between them (Fig. 2).

Aside from the well-defined features presented above, there also exist two broad absorption peaks around 1.6 and 2.2 eV. The same 1.6 eV peak was previously reported and correlated with electron spin resonance studies (ESR) of doped P3HT solutions.[19] This peak was attributed to bipolarons and believed to be the equilibrium charge-storage configuration in doped P3HT solutions. Furthermore the spin per charge approached zero when the doping level was higher than 1%, supporting the bipolaron hypothesis. Similar to ref. [20], we also observe a peak around 1.3 eV at lower doping concentration (1 mol%) (Fig. 1(c) inset). Since two polarons are needed to form a lower energy bipolaron, this state is favored at lower temperatures and higher charge concentration. We therefore assign the 1.6 eV peak visible in the 10% solution in Fig. 1(c) to BP2 transitions related to bipolarons (Fig. 2(d)) and the absorption peak at ~1.3 eV, visible in the lower concentration 1% solution, to P2 transitions related to polarons (Fig. 2(b)). The peak at 2.2 eV is nearly identical in energy to the π-π transition in pristine P3HT films, and, therefore, is attributed to neutral P3HT aggregates. These P3HT segments have locally straight backbones, with extended conjugation length, resulting in a smaller bandgap than undoped, fully dissolved P3HT molecules. The same absorption feature was also observed in $NO^{+}PF6^{-}$ doped P3HT solutions and was recognized as undoped P3HT aggregates.[19]

The decomposition of F4TCNQ-doped P3HT solution absorption (A_{doped}) into five components can be summarized with the following expression:

$$A_{Tot} = C_{P3HT}^{(T)} A_{P3HT}^{o} + C_{F4TCNQ}^{(T)} A_{F4TCNQ}^{o} + \left(1 - C_{F4TCNQ}^{(T)}\right) K_{BP}^{(T)} A_{BP}^{o} + K_{agg}^{(T)} A_{agg}^{o} + \left(1 - C_{F4TCNQ}^{(T)}\right) K_{F4-}^{(T)} A_{F4-}^{o} \quad (1)$$

Here A_{Tot} represents the total absorption spectrum containing contributions from all molecular species. $C_{P3HT}^{(T)}$ and $C_{F4TCNQ}^{(T)}$ represent the fractions of P3HT monomers and

F4TCNQ molecules that are neither charged nor aggregated at a particular quasi-steady state temperature. In addition, for each spectrum the A^o_{BP} and A^o_{agg} are the absorption of bipolarons and aggregated P3HT. $K^{(T)}_{BP}$, $K^{(T)}_{agg}$ and $K^{(T)}_{F4-}$ are the scaling factors for the normalized spectra of bipolarons, aggregated P3HT, and negatively charged F4TCNQ anions (extracted from ref. [20]). Note that the absorption signal of bipolarons (A^o_{BP}) and aggregated P3HT (A^o_{agg}) are represented as two normalized Gaussians where the peak positions and widths are constant for all spectra. Since the aggregate absorption does not dominate the energy region from 1.8-2.4 eV, we cannot apply the Spano model developed for P3HT.[26] Finally, A^o_{P3HT} and A^o_{F4TCNQ} represent the absorption of pure, neutral P3HT and F4TCNQ at the same concentration as the blend solution. All absorption spectra are fitted at the same time. The concentrations of neutral P3HT and F4TCNQ are calculated from $C^{(T)}_{P3HT}$ and $C^{(T)}_{F4TCNQ}$ while $K^{(T)}_{BP}$ is used to determine the absorption cross-section for bipolarons.

The fit summary shows, firstly, that there is a linear relationship between neutral P3HT monomer concentration (as a sum of both isolated molecules and aggregates) and F4CNQ anion concentration (Fig. 1(d)). Linear regression results reveal an estimate of ~4.9 bleached P3HT monomers for every negatively charged F4TCNQ anion molecule, which is also supported by the theoretical study from P. Pingel *et. al*.[27] Both high molecular weight (High MW, Mw= 108 kDa) and low molecular weight (Low MW, Mw=22-25 kDa) P3HT macromolecules were studied, as summarized in Table I. The bipolaron absorption peaks in these two P3HTs are very similar, with the peak centered around 1.64 eV and absorption cross-sections of 7×10^{-17} cm^2/charge, i.e. 3.5×10^{-17} cm^2/bipolaron. Finally, $K^{(T)}_{F4-}$ is used to extract the absorption cross-section for F4TCNQ anions and allows us to calculate the F4TCNQ anion concentration in thin films, presented in the following section of this paper.

Summarizing the previous paragraph: The efficiency with which F4TCNQ ionizes P3HT in solution can be controlled by the processing temperature. We found that sub-bandgap absorption signals in this system are mainly from F4TCNQ anions, P3HT bipolarons and P3HT aggregates. Our fitting suggests each F4TCNQ anion bleaches the absorption from

4.9 P3HT neutral monomers, and the peak intensity cross section of bipolarons is 7×10^{-17} cm^2/charge.

II. Doping in thin films

P3HT films with different doping concentrations (1wt% - 10wt%) were spin cast from hot (80°C) chlorobenzene solutions. This higher temperature ensures proper dissolution of the dopant-polymer complex and has been shown to not lead to volatilization of the F4TCNQ molecules.[24] To avoid spectral deformation in the absorption edge and subgap spectral region due to light scattering effects, absorption spectra were taken with an integrating sphere. The results are summarized in Fig. 3(a). As shown, P3HT films also exhibit bleached π-π absorption and an increase in sub-bandgap absorption upon introduction of the dopant. However, an absorption peak at ~1.3 eV is clearly observed in the doped films, appearing as a well-resolved shoulder on the low-energy side of the F4TCNQ anion absorption (inset in Fig. 3(a)), which is identified clearly as it is essentially identical as in solution. Hence, UV-visible spectra for thin films in the energy range of 1-2.5 eV can be decomposed into contributions from P3HT aggregates, F4TCNQ anions, and two Gaussian peaks centered around 1.3 and 1.6 eV. The spectra from neutral F4TCNQ and amorphous P3HT are not included here because their absorption signals appear above 2.5 eV (Fig. 1(a)), which is not in the energy range of interest. Similar to doped solutions, the decomposition of doped film spectra (inset in Fig. 3(a)) suggests that integer electron transfer is also observed in thin films based on the observation of the F4TCNQ anion signal.

The F4TCNQ anion signal in the UV-visible region can be used to estimate the doping efficiency in F4TCNQ-doped P3HT, assuming that all of the electrons in F4TCNQ anions are due to charge transfer from P3HT molecules. In Fig. 3(b), the two dimensional (2D) density of F4TCNQ anions ($[F4TCNQ]^-$), defined as number of charges per unit projected area in the film, was plotted as a function of total F4TCNQ molecule density, including both neutral ($[F4TCNQ]^0$) and negatively charged species ($[F4TCNQ]^-$). The total molecule density of F4TCNQ was calculated based on doping concentrations in

solution and the thickness of individual films, with the assumption that F4TCNQ molecules are dispersed in the film. This assumption is supported by X-Ray diffraction measurements of F4TCNQ-doped P3HT films, which showed that no signals from F4TCNQ crystallites were observed until the doping concentration reached ~30 wt%.[13] From the results, we can see that the F4TCNQ anion density is linearly dependent on the total F4TCNQ density. From a linear fit we find that within the doping concentration range of 1-10 wt%, 63% of F4TCNQ molecules are negatively ionized, in good agreement with previous work by P. Pingel and D. Neher.[21]

Two peaks, corresponding to charged P3HT, are identified at a lower energy, 1.3 eV (labeled polaron peak low: PPL) and at a higher energy, 1.6 eV (labeled polaron peak high: PPH), as shown in Fig. 1(a) inset, from the decomposition of film spectra with different doping concentrations. Their intensities are extracted and plotted as a function of F4TCNQ anion 2D density (Fig. 3(c)). Based on charge conservation, the positive charge density in P3HT must be equal to the negative charge density in F4TCNQ. From Fig. 3(c), we can see that both PPL and PPH peak intensities are proportional to the 2D charge density in P3HT. The detailed linear fit parameters for these two peaks are summarized in Table II. Note that the linear fit passes through the origin. The absorption peaks (PPL and PPH) are centered at 1.33 and 1.67 eV, with a full width at half maximum (FWHM) of 0.29 and 0.42 eV and absorption cross sections of 6.8×10^{-17} and 11.2×10^{-17} cm^2, respectively.

In order to further understand the form of charge carriers in F4TCNQ doped P3HT, the FTIR spectra of films with different doping concentrations were measured, as shown in Fig. 3(d). An integrating sphere could not be used in these measurements due to experimental limitations. Therefore, the absorption, especially in the region within P3HT's bandgap, is overestimated. Nevertheless, only one peak, centered at 0.55 eV, exists in the IR region > 0.5 eV. We label this spectral feature polaron IR peak (PIR). The absorption in far IR region, though not shown here, was also measured, but no absorption peak was observed down to ~0.2 eV. Although we are not able to measure accurately the peak intensity cross section/charge of PIR, we estimate it to be similar to that of PPL due

to the fact that the intensity of the PIR peak is very close to that of the shoulder (marked with an arrow in Fig. 3(a) insert) from PPL, as illustrated with a dotted line in Fig. 3(d). To summarize, three absorption peaks in the sub-bandgap region were observed and identified as absorptions from positively charged P3HT, which are possibly from polarons, bipolarons, 2D polarons or mixtures of these species.

The relative stability of polarons and bipolarons is a complicated problem in charged P3HT films. Some studies suggest that charge carriers in P3HT films are mainly bipolarons,[28,29] while others support the existence of mostly polarons.[20,30] If bipolarons were the only charge carriers in our F4TCNQ doped P3HT system, only two absorption peaks would be expected in the UV-vis and IR region. Since we observe three distinct peaks, we conclude that charge carriers consist of mainly polarons or 2D polarons, with possibly some bipolarons, while we can exclude that bipolarons are the only species. Previously, photoinduced absorption (PIA)[31–33] and charge modulation spectroscopy (CMS)[30,34,35] have been used to characterize optical absorption in charged P3HT. In the IR region, absorption peaks with energy lower than 0.2 eV were observed in both cases in regio-regular P3HT.[31,35] These peaks were identified as delocalized or 2D polarons, with energies much smaller than our IR absorption. On the other hand, absorption around 0.5 eV observed in PIA of regio-random P3HT was assigned to the P1 transition (Fig. 2).[31] A similar signal also appeared as a shoulder at 0.6 eV in CMS measurements within the IR region but was not discussed.[35] As a result, we exclude the existence of 2D polarons in our F4TCNQ doped P3HT and propose that polarons in this system prefer to localize on single P3HT chains. Therefore, charge carriers in F4TCNQ doped P3HT films can only be polarons, or a combination of polarons and bipolarons. If the absorption peaks, PPL and PPH, are from polarons and bipolarons, we would expect there to be an equilibrium between these two species ($P^+ + P^+ \leftrightharpoons BP^{2+}$). At higher charge concentrations, this equilibrium would be driven to the right-hand side, which implies that the signal from bipolarons would be stronger than that from polarons in more heavily doped films. However, our measurements show that peak intensities in both cases depend linearly on dopant density (Fig. 3(c)). Thus we attribute the three absorption peaks in our F4TCNQ-doped P3HT films to the P1, P2, and P3 transitions from P3HT polarons (Fig. 2(b)).

The existence of localized polarons is also supported by the microstructure of the P3HT/F4TCNQ system. On one hand, as shown in Fig. 3(a), upon doping, the ratio of 0-0 to 0-1 intensities increases compared with neat P3HT, which suggests that the incorporation of F4TCNQ molecules into P3HT aggregates lead to longer interaction lengths.[22,23] This observation can be attributed to the increase in chain rigidity resulting from interactions between F4TCNQ anions and P3HT cations, and is partially supported by the observation of the 2.3 eV peak in doped solution spectra. Straighter chains would support intrachain polaron delocalization and hinder interchain delocalization. This is in agreement with previous works by Ma et al.[14] On the other hand, XRD studies suggest the existence of P3HT and F4TCNQ co-crystals[13] in F4TCNQ-doped P3HT films. Such a structure, where F4TCNQ molecules are sandwiched between neighboring P3HT chains, makes it difficult for polarons/bipolarons to be delocalized over multiple chains. As a result, we believe that F4TCNQ-doped P3HT has a microstructure similar to that illustrated in Fig. 4(b), as previously described in Reference 13. Within the proposed microstructure, polarons should prefer to localize on only one P3HT chain and supports the reason why 2D polarons are not observed in our absorption measurement.

III. Measurement of background charge concentration in nominally intrinsic P3HT

With the quantitative knowledge of the absorption cross-section of single polarons we can now proceed to determine the level of background charge concentration in neat P3HT in the absence of intentional doping. While it is known that thin films of as-cast P3HT contain a certain level of charges due to unwanted background doping,[36] a direct measurement of residual charge density has never been attempted. Taking advantage of the exceptional sensitivity of Photothermal Deflection Spectroscopy (PDS), we measured weak absorption signals from polarons around 1.3 eV in thin films of pure P3HT having different molecular weight and processed from 2 different solvents (Fig. 5). The PDS cells were loaded and sealed in a glovebox with low oxygen contents (<5 ppm).

Therefore our measurements are representative of P3HT films kept in an inert environment during their processing. Exposure to air is known to dope P3HT. However the sub-bandgap signals shown in Fig. 5 were stable over days suggesting that no atmospheric contamination was occurring during the measurement. Using the peak positions and FHWM listed in Table II, we are able to extract the PPL peak intensity in neat P3HT films from an exponential decay background. The polaron densities in these three films are estimated to be 8.1×10^{16} cm^{-3}, 4.1×10^{16} cm^{-3} and 4.5×10^{16} cm^{-3}. As a comparison, 1.25 wt% F4TCNQ-doped P3HT exhibits a polaron density of ~3.2×10^{19} cm^{-3}. These initial measurements suggest that the background charge density is weakly dependent of microstructure or molecular weight. It should be noted that these figures correspond to the total polaron concentration. Neher et al. estimate that at low dopant concentration, approximately 5% of the charges are mobile.[21] We conclude that pure P3HT films contain mobile polarons in concentrations of the order of 10^{15} cm^{-3}, which is in agreement with what was observed by Pingel et al.[24] We note here that Liang and Gregg[36] observed a higher mobile hole density (~10^{-16} cm^{-3}), which may be a result of a less pure and lower regioregular batch of P3HT. Nevertheless, these calculations give us a reasonable estimate of the residual charge density inside pure P3HT films.[37]

In conclusion, UV-visible and IR absorption spectra of F4TCNQ-doped P3HT at different doping concentrations were measured and analyzed in both solutions and thin films. The absorption signatures from F4TCNQ, P3HT, F4TCNQ anions and P3HT cations are identified in doped P3HT solutions and films. We found that only singly charged F4TCNQ anions are observed in doped systems, indicating integral charge transfer between P3HT and F4TCNQ molecules. In solution, only one sub-gap absorption peak at 1.6 eV is observed, suggesting that the bipolarons are the main charged species in P3HT, with a cross section of 7×10^{-17} cm^2/charge. In addition, 63% of the dopants generate a P3HT cation in thin films. Furthermore, optical absorption and structural analysis suggest that the polaron in F4TCNQ doped P3HT is mainly localized on 1D polymer chains. P3HT polaron cross sections in the UV-visible region were calculated to be $7 \times 10^{-17} cm^2$ and 1×10^{-16} cm^2, which allows for the estimation of residual charge densities in 'pure' P3HT films.

Acknowledgments: D.T.D thanks the support of the Stanford Graduate Fellowship and the National Science Foundation Graduate Research Fellowship. Financial support from the National Science Foundation (DMR 1205752) is gratefully acknowledged.

References

[1] J. Blochwitz, M. Pfeiffer, T. Fritz, and K. Leo, Appl. Phys. Lett. **73**, 729 (1998).

[2] K. Walzer, B. Maennig, M. Pfeiffer, and K. Leo, Chem. Rev. **107**, 1233 (2007).

[3] X. Zhou, J. Blochwitz, M. Pfeiffer, A. Nollau, T. Fritz, and K. Leo, Adv. Funct. Mater. **11**, 310 (2001).

[4] T. Taima, J. Sakai, T. Yamanari, and K. Saito, Sol. Energy Mater. Sol. Cells **93**, 742 (2009).

[5] K.-H. Yim, G.L. Whiting, C.E. Murphy, J.J.M. Halls, J.H. Burroughes, R.H. Friend, and J.-S. Kim, Adv. Mater. **20**, 3319 (2008).

[6] Y. Zhang, B. de Boer, and P.W.M. Blom, Adv. Funct. Mater. **19**, 1901 (2009).

[7] P. Pingel, R. Schwarzl, and D. Neher, Appl. Phys. Lett. **100**, 143303 (2012).

[8] M. Pfeiffer, A. Beyer, T. Fritz, and K. Leo, Appl. Phys. Lett. **73**, 3202 (1998).

[9] W. Gao and A. Kahn, J. Appl. Phys. **94**, 359 (2003).

[10] M.D. Irwin, D.B. Buchholz, A.W. Hains, R.P.H. Chang, and T.J. Marks, Proc. Natl. Acad. Sci. **105**, 2783 (2008).

[11] L. Zhu, E. Kim, Y. Yi, and J. Bredas, Chem. Mater. **23**, 5149 (2011).

[12] I. Salzmann, G. Heimel, S. Duhm, M. Oehzelt, P. Pingel, B.M. George, A. Schnegg, K. Lips, R.-P. Blum, A. Vollmer, and N. Koch, Phys. Rev. Lett. **108**, 035502 (2012).

[13] D.T. Duong, C. Wang, E. Antono, M.F. Toney, and A. Salleo, Org. Electron. Physics, Mater. Appl. **14**, 1330 (2013).

[14] L. Ma, W.H. Lee, Y.D. Park, J.S. Kim, H.S. Lee, and K. Cho, Appl. Phys. Lett. **92**, 063310 (2008).

[15] M. Lehnhardt, S. Hamwi, M. Hoping, J. Reinker, T. Riedl, and W. Kowalsky, Appl. Phys. Lett. **96**, 193301 (2010).

[16] M.L. Tietze, L. Burtone, M. Riede, B. Lüssem, and K. Leo, Phys. Rev. B **86**, 035320 (2012).

[17] S. Olthof, W. Tress, R. Meerheim, B. Lu□ssem, and K. Leo, J. Appl. Phys. **106**, 103711 (2009).

[18] F. Maddalena, E.J. Meijer, K. Asadi, D.M. de Leeuw, and P.W.M. Blom, Appl. Phys. Lett. **97**, 043302 (2010).

[19] N. Colaneri, M. Nowak, D. Spiegel, S. Hotta, and A.J. Heeger, Phys. Rev. B **36**, 7964 (1987).

[20] K.E. Ziemelis, A.T. Hussain, D.D.C. Bradley, R.H. Friend, J. Ruhe, and G. Wegner, Phys. Rev. Lett. **66**, 2231 (1991).

[21] P. Pingel and D. Neher, Phys. Rev. B **87**, 115209 (2013).

[22] J. Gao, E.T. Niles, and J.K. Grey, (2013).

[23] J. Gao, J.D. Roehling, Y. Li, H. Guo, A.J. Moulé, and J.K. Grey, J. Mater. Chem. C **1**, 5638 (2013).

[24] D.T. Duong, H. Phan, D. Hanifi, P.S. Jo, T.-Q. Nguyen, and A. Salleo, Adv. Mater. **26**, 6069 (2014).

[25] J.B. Torrance, J.J. Mayerle, K. Bechgaard, B.D. Silverman, and Y. Tomkiewicz, Phys. Rev. B **22**, 4960 (1980).

[26] S.T. Turner, P. Pingel, R. Steyrleuthner, E.J.W. Crossland, S. Ludwigs, and D. Neher, Adv. Funct. Mater. **21**, 4640 (2011).

[27] P. Pingel, L. Zhu, K.S. Park, J.-O. Vogel, S. Janietz, E.-G. Kim, J.P. Rabe, J.-L. Brédas, and N. Koch, J. Phys. Chem. Lett. **1**, 2037 (2010).

[28] M.J. Nowak, D. Spiegel, S. Hotta, A.J. Heeger, and P.A. Pincus, Macromolecules **22**, 2917 (1989).

[29] N. Sai, Z. Li, M. Martin, D. Basov, and M. Di Ventra, Phys. Rev. B **75**, 045307 (2007).

[30] P. Brown, H. Sirringhaus, M. Harrison, M. Shkunov, and R. Friend, Phys. Rev. B **63**, 125204 (2001).

[31] R. Österbacka, C.P. An, X.M. Jiang, and Z.V. Vardeny, Science (80-.). **287**, 839 (2000).

[32] B.X. Jiang, R. Österbacka, O. Korovyanko, C.P. An, B. Horovitz, R.A.J. Janssen, and Z.V. Vardeny, Adv. Funct. Mater. **12**, 587 (2002).

[33] O. Korovyanko, R. Österbacka, X. Jiang, Z. Vardeny, and R. Janssen, Phys. Rev. B **64**, 235122 (2001).

[34] P. Brown, D. Thomas, A. Köhler, J. Wilson, J.-S. Kim, C. Ramsdale, H. Sirringhaus, and R. Friend, Phys. Rev. B **67**, 064203 (n.d.).

[35] J.-F. Chang, J. Clark, N. Zhao, H. Sirringhaus, D. Breiby, J. Andreasen, M. Nielsen, M. Giles, M. Heeney, and I. McCulloch, Phys. Rev. B **74**, 115318 (2006).

[36] Z. Liang and B. a Gregg, Adv. Mater. **24**, 3258 (2012).

[37] C.G. Shuttle, N.D. Treat, J.D. Douglas, J.M.J. Fréchet, and M.L. Chabinyc, Adv. Energy Mater. **2**, 111 (2012).

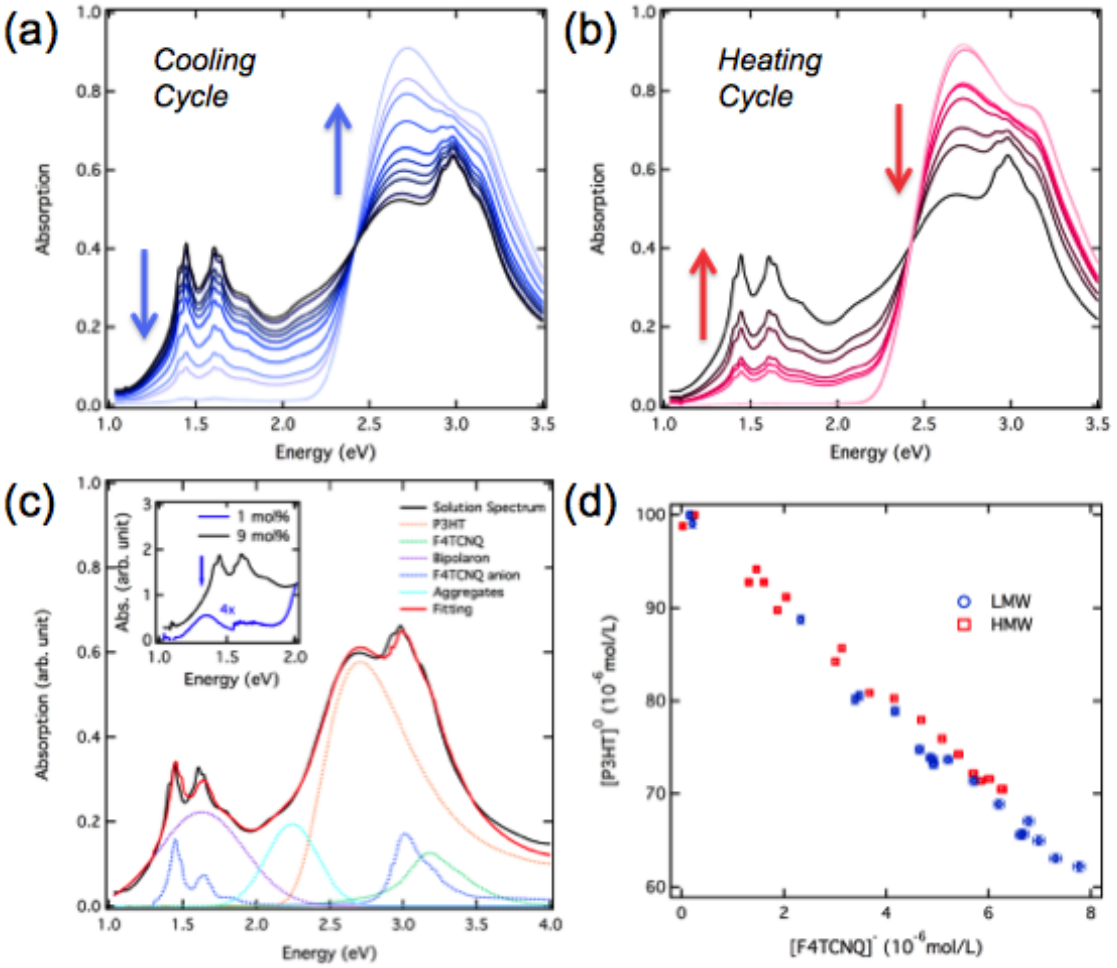

FIG. 1. UV-vis spectra of a F4TCNQ doped P3HT solution (9 mol%), within (a) cooling and (b) heating cycles. (c) Example of a solution doped absorption spectrum, decomposed into: absorption from neutral P3HT and F4TCNQ in solution, P3HT aggregates, F4TCNQ anion, and Gaussian peaks centered around 1.3 eV and 1.6 eV (inset: 1 mol% and 9 mol% solution spectra in the sub-bandgap region). The 1.3 eV peak is overwhelmed by the 1.6 eV peak at high concentrations and cannot be fitted independently. Molar content of neutral P3HT monomers as a function of F4TCNQ anions, derived from the spectral decomposition in low molecular-weight (LMW) and high molecular-weight (HMW) P3HT (d). Note that all absorption spectra are collected at room temperatures.

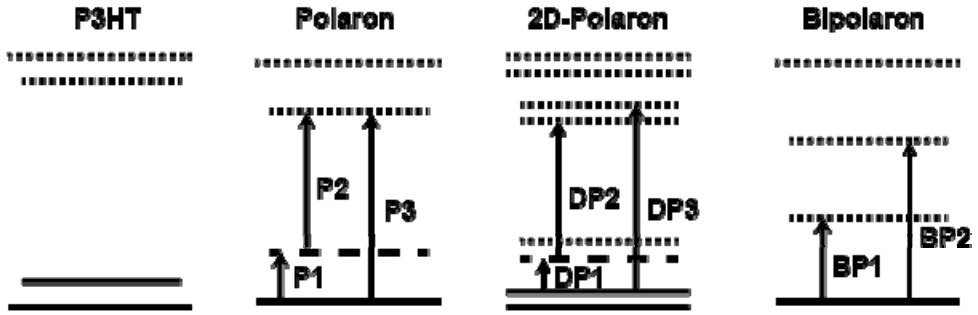

FIG. 2. Energy levels and transitions in charged and neutral P3HT: (a) neutral P3HT, (b) polaron, (c) 2D-polaron, which is not likely to be present in large quantities in solutions of well-dissolved P3HT, and (d) bipolarons. The solid, dashed and dotted lines represent fully-occupied, half-occupied and empty states, respectively.

	Peak Energy (eV)	FWHM (eV)	Peak intensity cross section (cm^2/charge)
High MW	1.63	0.67	7.3×10^{-17}
Low MW	1.65	0.68	7.1×10^{-17}

TABLE I. Bipolaron peak properties in F4TCNQ doped P3HT solutions.

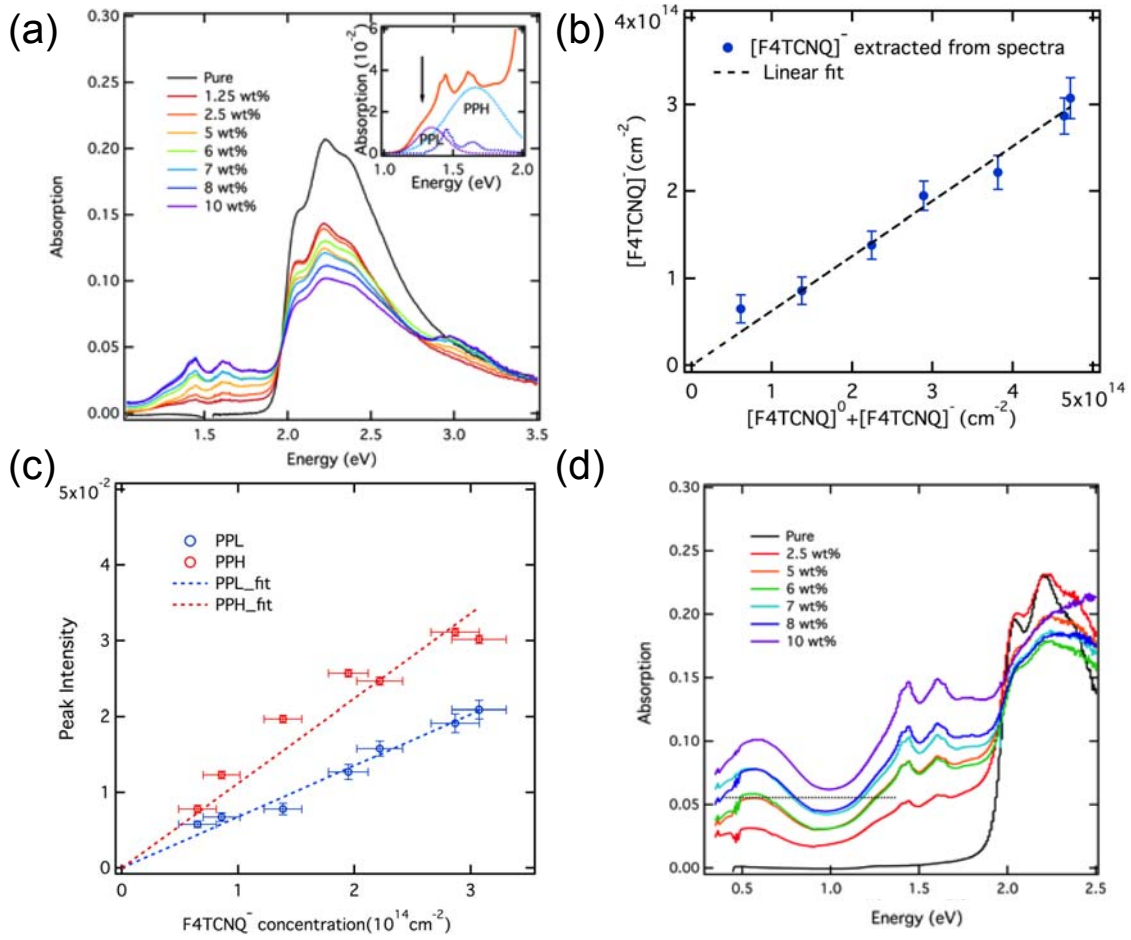

FIG. 3. (a) UV-vis spectra of F4TCNQ doped P3HT thin films with varying doping concentrations, and (inset) spectral decomposition in the sub-bandgap region, with two Gaussian peaks centered at 1.3 eV and 1.6 eV, labeled PPL and PPH, respectively. (b) Ionized F4TCNQ as a function of total F4TCNQ concentration (c) Peak intensity of PPL and PPH as a function of 2D density of F4TCNQ anion $[F4TCNQ]^-$ (d) FTIR spectra of P3HT/F4TCNQ films with different doping densities.

TABLE II. Properties of polaron peaks in F4TCNQ doped P3HT film

	Peak Energy (eV)	FWHM (eV)	Peak Intensity Cross Section (cm^2/charge)
PPL	1.33	0.29	$(6.8\pm0.2)\times10^{-17}$
PPH	1.67	0.42	$(11.2\pm0.6)\times10^{-17}$

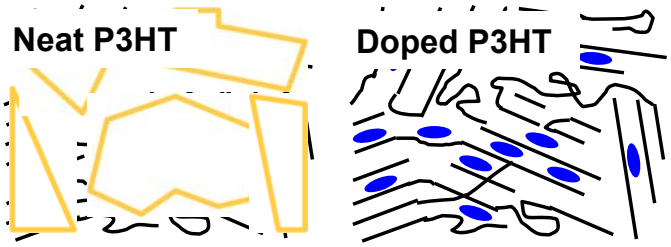

FIG. 4. Illustration of the microstructures in (a) pristine and (b) doped P3HT films

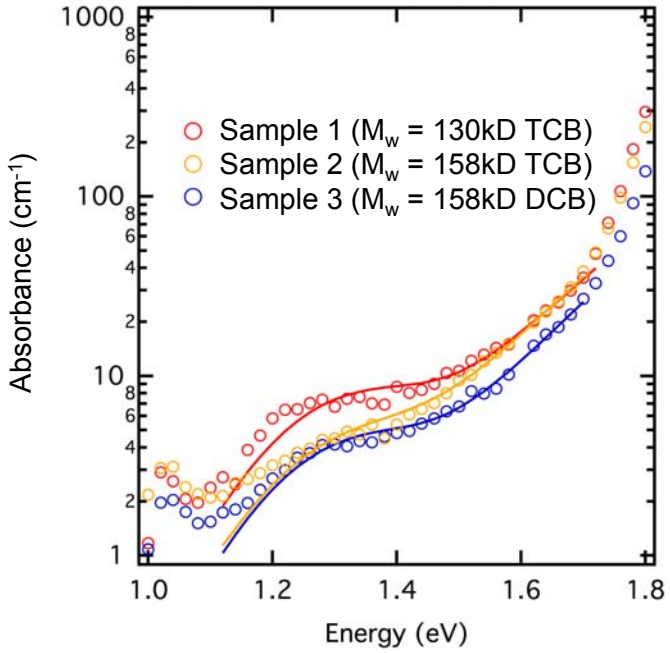

FIG. 5. PDS spectrum in the subgap region of neat P3HT thin films with different MWs and prepared with different casting solvents (DCB=dichlorobenzene; TCB=trichlorobenzene).